Impact of half-wave plate systematics on the observed CMB polarization

Marta Monelli
Max Planck Institut für Astrophysik
Garching (Germany)

CMB Group Meeting, *KEK*, June 21st, 2023

CMB anisotropies

Inhomogeneities at photon decoupling imprint anisotropies on the CMB.

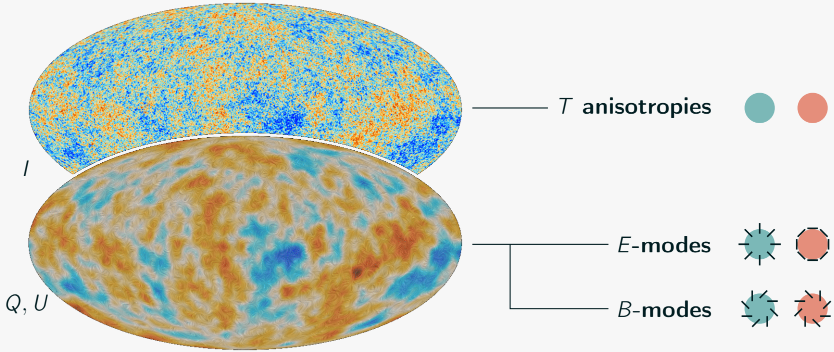

image credit: Jonathan Aumont

CMB anisotropies

Inhomogeneities at photon decoupling imprint anisotropies on the CMB.

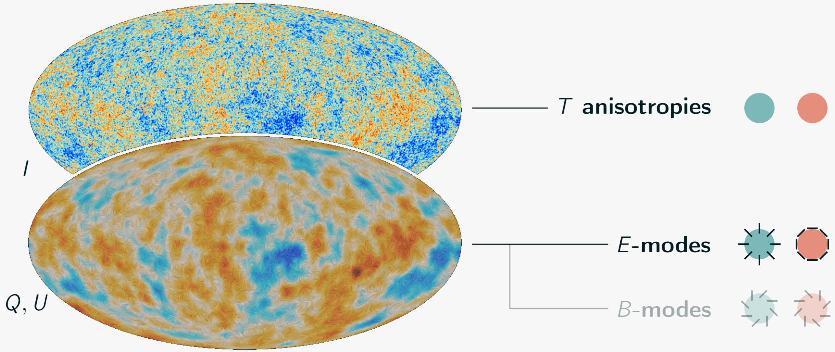

image credit: Jonathan Aumont

searching for B-modes

- **Inflation**-sourced tensor perturbations are expected to leave a distinctive signature (B-modes) on CMB polarization:

$$C_\ell^{BB} = rC_\ell^{\mathrm{GW}} + C_\ell^{\mathrm{lensing}}\,.$$

This is driving the development of a number of new missions:

- ☐ Simons Observatory,
- ☐ South Pole Observatory,
- ☐ CMB Stage-4,
- ☐ **LiteBIRD**.

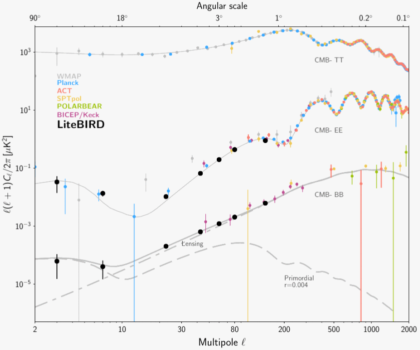

image credit: LiteBIRD Collaboration (2022) PTEP

measuring polarization

describing polarization: Stokes vectors

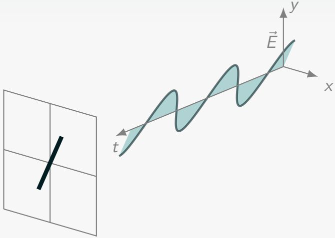

linearly polarized

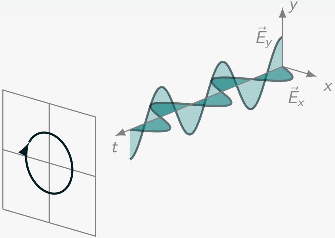

circularly polarized

$$\text{Stokes vector } \vec{S} \equiv \begin{pmatrix} I \\ Q \\ U \\ V \end{pmatrix} \equiv \begin{pmatrix} |E_x|^2 + |E_y|^2 \\ |E_x|^2 - |E_y|^2 \\ 2\mathrm{Re}(E_x E_y^*) \\ -2\mathrm{Im}(E_x E_y^*) \end{pmatrix}$$

describing polarization: Stokes vectors

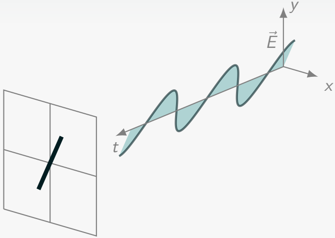

linearly polarized

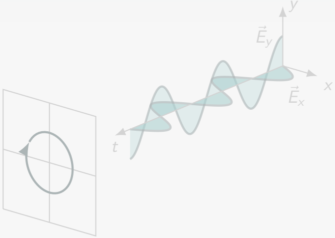

circularly polarized

$$\text{Stokes vector } \vec{S} \equiv \begin{pmatrix} I \\ Q \\ U \\ V \end{pmatrix} \equiv \begin{pmatrix} |E_x|^2 + |E_y|^2 \\ |E_x|^2 - |E_y|^2 \\ 2\mathrm{Re}(E_x E_y^*) \\ -2\mathrm{Im}(E_x E_y^*) \end{pmatrix}$$

describing polarization: Stokes vectors

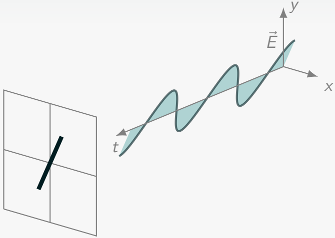

linearly polarized

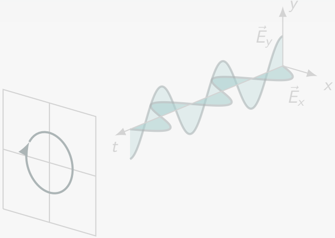

circularly polarized

$$\text{Stokes vector } \vec{S} \equiv \begin{pmatrix} I \\ Q \\ U \\ V \end{pmatrix} \equiv \begin{pmatrix} |E_x|^2 + |E_y|^2 \\ |E_x|^2 - |E_y|^2 \\ 2\mathrm{Re}(E_x E_y^*) \\ -2\mathrm{Im}(E_x E_y^*) \end{pmatrix}$$

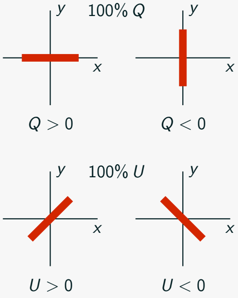

matrix methods for computing polarization

Mueller calculus: radiation described as $S = (I, Q, U)$, effect of polarization-altering devices parametrized by $\mathcal{M}$ so that $\mathsf{S}' = \mathcal{M} \cdot \mathsf{S}$.

$$\mathcal{M}_{\text{pol}} = \frac{1}{2}\begin{pmatrix} 1 & 1 & 0 \\ 1 & 1 & 0 \\ 0 & 0 & 0 \end{pmatrix}, \quad \mathcal{M}_\theta = \begin{pmatrix} 1 & 0 & 0 \\ 0 & \cos(2\theta) & \sin(2\theta) \\ 0 & -\sin(2\theta) & \cos(2\theta) \end{pmatrix}, \quad \ldots$$

Given two optical elements in series with $\mathcal{M}_1$ and $\mathcal{M}_2$, their combined effect can be described by $\mathcal{M}_2\mathcal{M}_1$.

Matrix methods are extremely convenient to manipulate polarization, since one does not work with the electromagnetic field itself.

an example: pair-differencing systematics

Polarization can be measured by comparing the readings of pairs of (orthogonal) detectors:

$$
\begin{aligned}
d_1 &= a \cdot \mathcal{M}_{\mathrm{pol}} \cdot S = \begin{pmatrix} 1 & 0 & 0 \end{pmatrix} \frac{1}{2} \begin{pmatrix} 1 & 1 & 0 \\ 1 & 1 & 0 \\ 0 & 0 & 0 \end{pmatrix} \begin{pmatrix} I \\ Q \\ U \end{pmatrix} = I + Q \,, \\
d_2 &= a \cdot \mathcal{M}_{\mathrm{pol}} \mathcal{M}_{\pi/2} \cdot S = I - Q \,.
\end{aligned}
$$

This method can lead to detection of spurious polarization.

the path forward

How will next generation CMB experiments deal with this?

- LiteBIRD,
- Simons Observatory,
- South Pole Observatory,
- CMB Stage-4.

the path forward

How will next generation CMB experiments deal with this?

- ☑ LiteBIRD,
- ☑ Simons Observatory,
- ☑ South Pole Observatory,
- ☑ CMB Stage-4.

They **all** plan to employ rotating **half-wave plates (HWPs)** as polarization modulators.

the HWP: reducing systematics

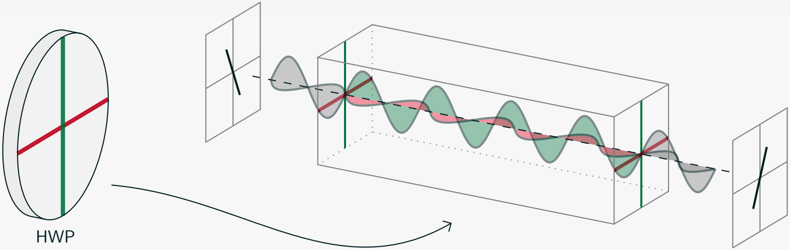

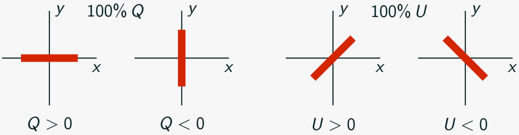

$$\mathcal{M}_{\text{HWP}} = \begin{pmatrix} 1 & 0 & 0 \\ 0 & 1 & 0 \\ 0 & 0 & -1 \end{pmatrix}$$

A **rotating** half-wave plate (HWP) as first optical element can help to control systematics.

ideal rotating HWP

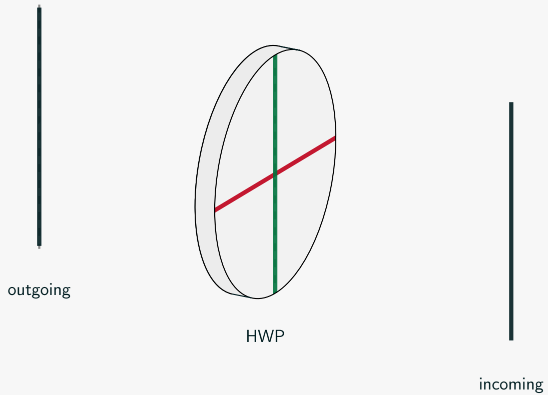

ideal rotating HWP

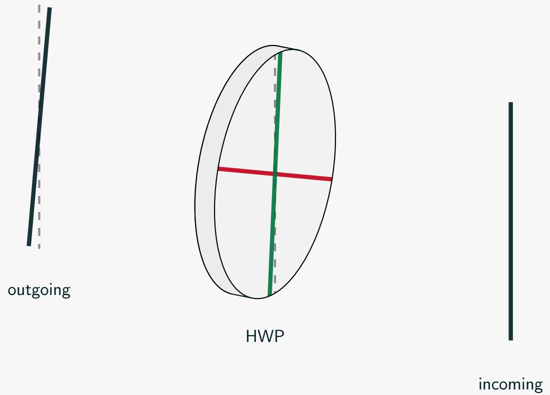

ideal rotating HWP

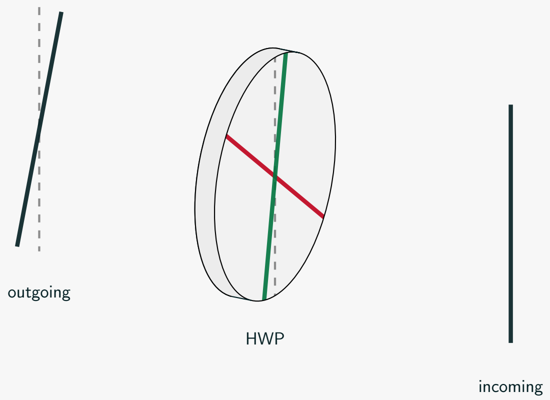

ideal rotating HWP

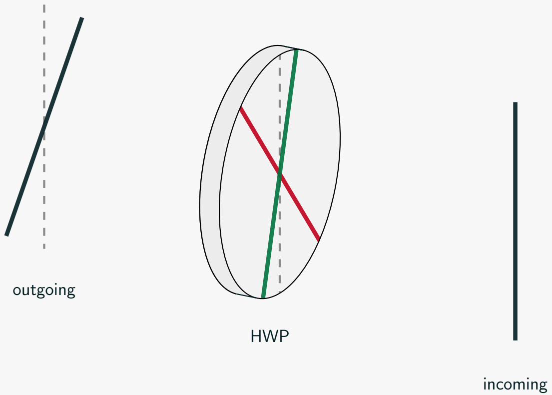

ideal rotating HWP

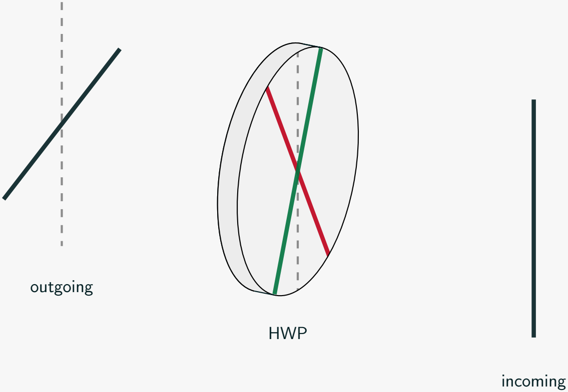

ideal rotating HWP

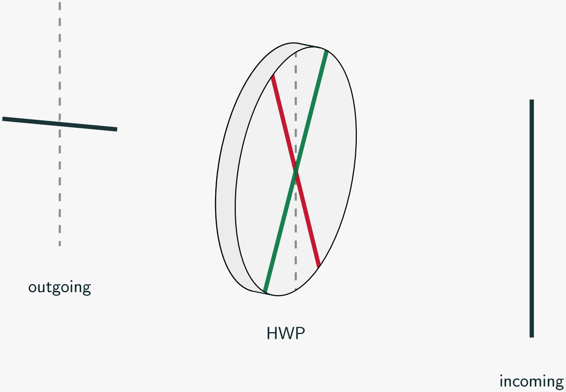

ideal rotating HWP

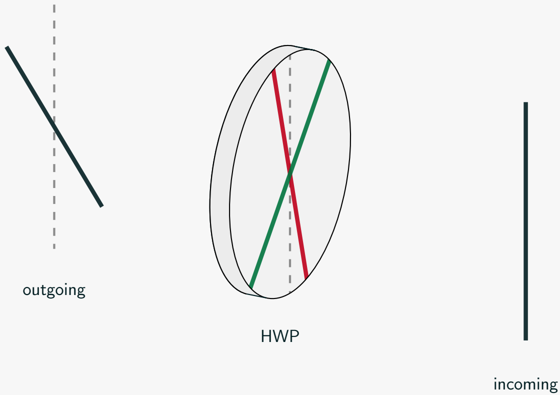

ideal rotating HWP

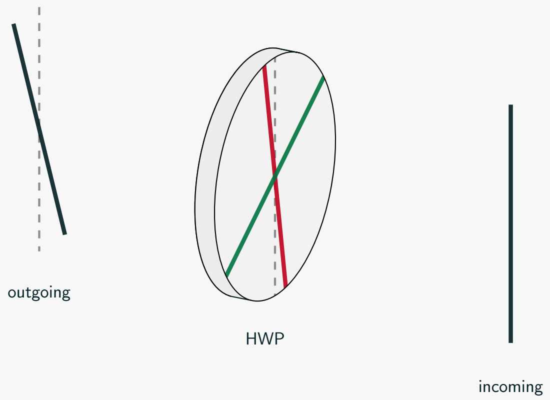

ideal rotating HWP

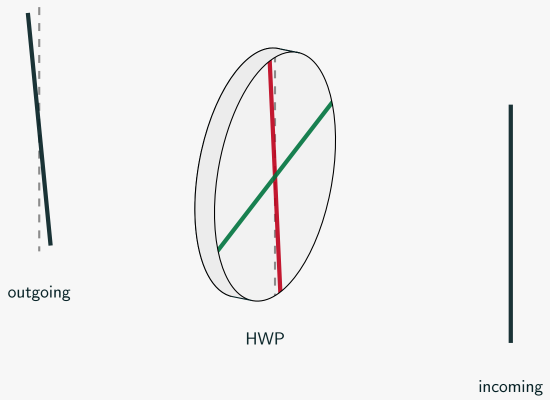

ideal rotating HWP

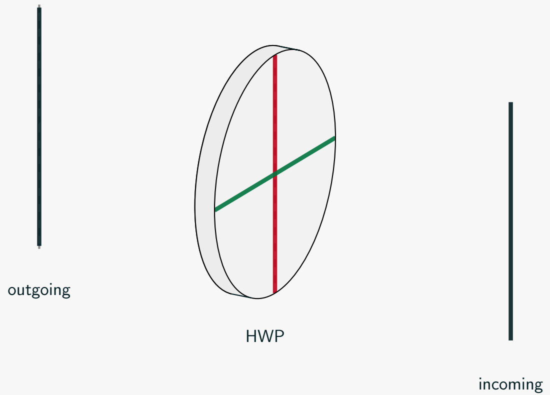

ideal rotating HWP

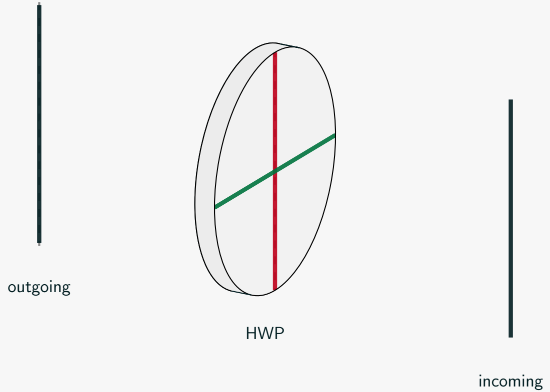

- The intrinsic signal is modulated to $4f_{\mathbf{HWP}}$ and can be distinguished from spurious signal (no/different modulation).

the HWP Mueller matrix

For an ideal HWP, $\mathcal{M}_{\text{HWP}}$ is simply $\mathcal{M}_{\text{ideal}} = \text{diag}(1, 1, -1)$, but things get more complicated for realistic cases:

$$\mathcal{M}_{\text{HWP}} = \left(\quad \right).$$

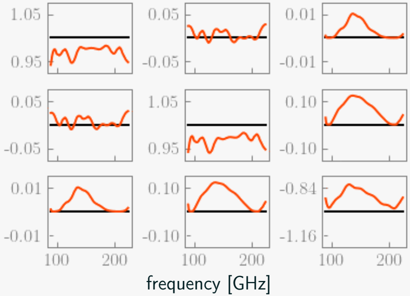

How does this affect the observed maps?

Giardiello et al. (2022) A&A 658

simulating/modeling the HWP effect

how to propagate systematics

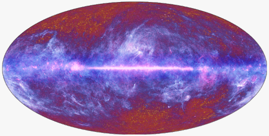

CMB sky maps

image credit: *Planck* collaboration

how to propagate systematics

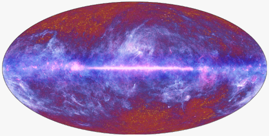

detection

time ordered data (TOD)

map-making

multi-frequency maps

foreground cleaning

CMB sky maps

TOD: collection of the signal detected by *each of the (4508) detectors* during *the whole (3-year) mission*.

image credit: *Planck* collaboration

how to propagate systematics

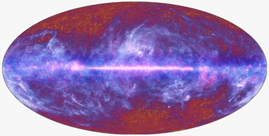

detection

time ordered data (TOD)

map-making

multi-frequency maps

foreground cleaning

CMB sky maps

TOD: collection of the signal detected by *each of the (4508) detectors* during *the whole (3-year) mission*.

Simulating and **modeling** TOD is crucial in the planning of any CMB experiment: it helps studying potential systematic effects.

image credit: *Planck* collaboration

simulating vs modeling

Realistic simulations are key for the study of systematics, because they can account for them in their (at least partial) complexity.

Approximate models, on the other hand, are extremely useful to gain some intuition about the problem at hand.

simulating vs modeling

Realistic simulations are key for the study of systematics, because they can account for them in their (at least partial) complexity.

Approximate models, on the other hand, are extremely useful to gain some intuition about the problem at hand.

Just in case, we did **both**.

beamconv-**based simulation pipeline**

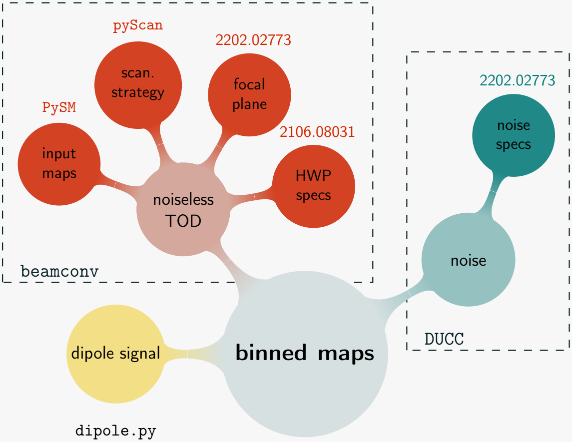

github.com/AdriJD/beamconv, A. Duivenvoorden et al "2012.10437", gitlab.mpcdf.mpg.de/mtr/ducc

modeling: working assumptions

To focus on the impact of **HWP non-idealities** we consider a simplified problem:

- no noise,
- single frequency,
- CMB-only,
- simple beams,
- HWP aligned to the detector line of sight.

modeling the TOD

(minimal) TOD: signal detected by 4 detectors.

$$\begin{pmatrix} d^{(0)} \\ d^{(90)} \\ d^{(45)} \\ d^{(135)} \end{pmatrix} = \begin{pmatrix} (1\ 1\ 0) \cdot \mathcal{R}_{0-\phi} \mathcal{M}_{\text{HWP}} \mathcal{R}_{\phi+\psi} \\ (1\ 1\ 0) \cdot \mathcal{R}_{90-\phi} \mathcal{M}_{\text{HWP}} \mathcal{R}_{\phi+\psi} \\ (1\ 1\ 0) \cdot \mathcal{R}_{45-\phi} \mathcal{M}_{\text{HWP}} \mathcal{R}_{\phi+\psi} \\ (1\ 1\ 0) \cdot \mathcal{R}_{135-\phi} \mathcal{M}_{\text{HWP}} \mathcal{R}_{\phi+\psi} \end{pmatrix} \cdot \begin{pmatrix} I_{\text{in}} \\ Q_{\text{in}} \\ U_{\text{in}} \end{pmatrix}$$

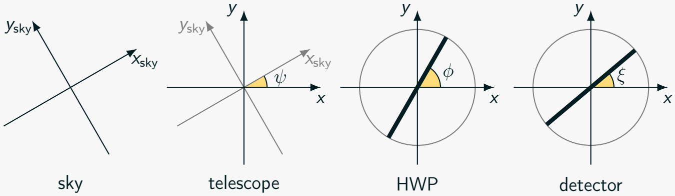

modeling the TOD

(minimal) TOD: signal detected by 4 detectors.

$$\begin{pmatrix} d^{(0)} \\ d^{(90)} \\ d^{(45)} \\ d^{(135)} \end{pmatrix} = \underbrace{\begin{pmatrix} (1\ 1\ 0) \cdot \mathcal{R}_{0-\phi}\mathcal{M}_{\mathrm{HWP}}\mathcal{R}_{\phi+\psi} \\ (1\ 1\ 0) \cdot \mathcal{R}_{90-\phi}\mathcal{M}_{\mathrm{HWP}}\mathcal{R}_{\phi+\psi} \\ (1\ 1\ 0) \cdot \mathcal{R}_{45-\phi}\mathcal{M}_{\mathrm{HWP}}\mathcal{R}_{\phi+\psi} \\ (1\ 1\ 0) \cdot \mathcal{R}_{135-\phi}\mathcal{M}_{\mathrm{HWP}}\mathcal{R}_{\phi+\psi} \end{pmatrix}}_{\text{response matrix } A} \cdot \begin{pmatrix} I_{\mathrm{in}} \\ Q_{\mathrm{in}} \\ U_{\mathrm{in}} \end{pmatrix}$$

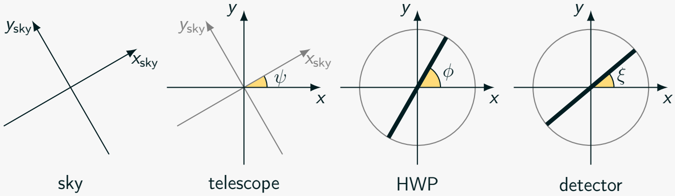

modeling the observed maps

map-maker: bin-averaging $\widehat{S} = (\widehat{A}^T \widehat{A})^{-1} \widehat{A}^T A \cdot S$ assuming ideal HWP.

$$\widehat{A} = \begin{pmatrix} (1\ 1\ 0) \cdot \mathcal{R}_{0-\phi} \mathcal{M}_{\text{ideal}} \mathcal{R}_{\phi+\psi} \\ (1\ 1\ 0) \cdot \mathcal{R}_{90-\phi} \mathcal{M}_{\text{ideal}} \mathcal{R}_{\phi+\psi} \\ (1\ 1\ 0) \cdot \mathcal{R}_{45-\phi} \mathcal{M}_{\text{ideal}} \mathcal{R}_{\phi+\psi} \\ (1\ 1\ 0) \cdot \mathcal{R}_{135-\phi} \mathcal{M}_{\text{ideal}} \mathcal{R}_{\phi+\psi} \end{pmatrix}$$

estimated ouput maps

$$\widehat{I} = m_{ii} I_{\rm in} + (m_{iq} Q_{\rm in} + m_{iu} U_{\rm in}) \cos(2\alpha) + (m_{iq} U_{\rm in} - m_{iu} Q_{\rm in}) \sin(2\alpha)\,,$$

$$\begin{aligned}\widehat{Q} = \frac{1}{2}\Big\{&(m_{qq} - m_{uu}) Q_{\rm in} + (m_{qu} + m_{uq}) U_{\rm in} + 2 m_{qi} I_{\rm in} \cos(2\alpha) + 2 m_{ui} I_{\rm in} \sin(2\alpha)\\ &+ \left[(m_{qq} + m_{uu}) Q_{\rm in} + (m_{qu} - m_{uq}) U_{\rm in}\right] \cos(4\alpha)\\ &+ \left[-(m_{qu} - m_{uq}) Q_{\rm in} + (m_{qq} + m_{uu}) U_{\rm in}\right] \sin(4\alpha)\Big\}\,,\end{aligned}$$

$$\begin{aligned}\widehat{U} = \frac{1}{2}\Big\{&(m_{qq} - m_{uu}) U_{\rm in} - (m_{qu} + m_{uq}) Q_{\rm in} - 2 m_{ui} I_{\rm in} \cos(2\alpha) + 2 m_{qi} I_{\rm in} \sin(2\alpha)\\ &+ \left[-(m_{qq} + m_{uu}) U_{\rm in} + (m_{qu} - m_{uq}) Q_{\rm in}\right] \cos(4\alpha)\\ &+ \left[(m_{qu} - m_{uq}) U_{\rm in} + (m_{qq} + m_{uu}) Q_{\rm in}\right] \sin(4\alpha)\Big\}\,,\end{aligned}$$

where $\alpha = \phi + \psi$. For **good** coverage and **rapidly spinning** HWP:

$$\widehat{\mathsf{S}} \simeq \begin{pmatrix} m_{ii} I_{\rm in} \\ [(m_{qq} - m_{uu}) Q_{\rm in} + (m_{qu} + m_{uq}) U_{\rm in}]/2 \\ [(m_{qq} - m_{uu}) U_{\rm in} - (m_{qu} + m_{uq}) Q_{\rm in}]/2 \end{pmatrix}.$$

Monelli et al. (2023) JCAP 03

angular power spectra

Expanding $\widehat{S}$ in spherical harmonics:

$$\widehat{C}_\ell^{TT} \simeq m_{ii}^2 C_{\ell,\text{in}}^{TT},$$

$$\widehat{C}_\ell^{EE} \simeq \frac{(m_{qq}-m_{uu})^2}{4} C_{\ell,\text{in}}^{EE} + \frac{(m_{qu}+m_{uq})^2}{4} C_{\ell,\text{in}}^{BB} + \frac{(m_{qq}-m_{uu})(m_{qu}+m_{uq})}{2} C_{\ell,\text{in}}^{EB},$$

$$\widehat{C}_\ell^{BB} \simeq \frac{(m_{qq}-m_{uu})^2}{4} C_{\ell,\text{in}}^{BB} + \frac{(m_{qu}+m_{uq})^2}{4} C_{\ell,\text{in}}^{EE} - \frac{(m_{qq}-m_{uu})(m_{qu}+m_{uq})}{2} C_{\ell,\text{in}}^{EB},$$

$$\widehat{C}_\ell^{TE} \simeq \frac{m_{ii}(m_{qq}-m_{uu})}{2} C_{\ell,\text{in}}^{TE} + \frac{m_{ii}(m_{qu}+m_{uq})}{2} C_{\ell,\text{in}}^{TB},$$

$$\widehat{C}_\ell^{EB} \simeq \frac{(m_{qq}-m_{uu})^2-(m_{qu}+m_{uq})^2}{4} C_{\ell,\text{in}}^{EB} - \frac{(m_{qq}-m_{uu})(m_{qu}+m_{uq})}{2} (C_{\ell,\text{in}}^{EE} - C_{\ell,\text{in}}^{BB}),$$

$$\widehat{C}_\ell^{TB} \simeq \frac{m_{ii}(m_{qq}-m_{uu})}{2} C_{\ell,\text{in}}^{TB} - \frac{m_{ii}(m_{qu}+m_{uq})}{2} C_{\ell,\text{in}}^{TE}.$$

Monelli et al. (2023) JCAP 03

analytical vs simulated output spectra

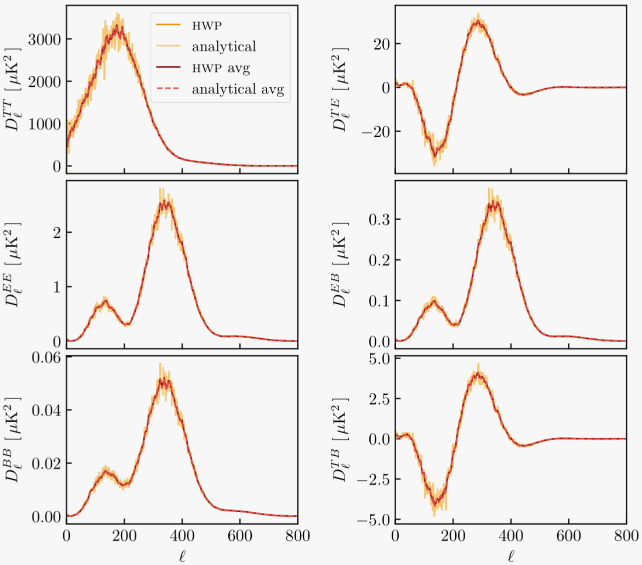

Monelli et al. (2023) JCAP 03

a first application:
impact on cosmic birefringence

cosmic birefringence in harmonic space

Rotation of the plane of linear polarization of photons travelling through a time dependent pseudoscalar field.

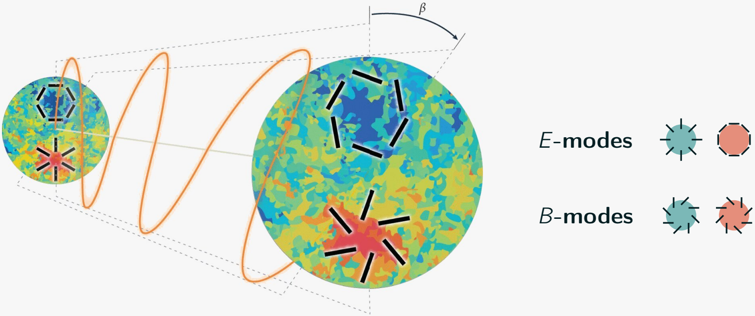

Mixing of E and B modes: $$\begin{cases} a^E_{\ell m,\mathrm{obs}} = a^E_{\ell m}\cos 2\beta - a^B_{\ell m}\sin 2\beta, \\ a^B_{\ell m,\mathrm{obs}} = a^E_{\ell m}\sin 2\beta + a^B_{\ell m}\cos 2\beta. \end{cases}$$

image credit: Yuto Minami

hints of cosmic birefringence

$$\begin{cases} C_{\ell,\mathrm{obs}}^{TT} = C_\ell^{TT}, \\ C_{\ell,\mathrm{obs}}^{EE} = \cos^2(2\beta) C_\ell^{EE} + \sin^2(2\beta) C_\ell^{BB} - \sin(4\beta) C_\ell^{EB}, \\ C_{\ell,\mathrm{obs}}^{BB} = \cos^2(2\beta) C_\ell^{BB} + \sin^2(2\beta) C_\ell^{EE} + \sin(4\beta) C_\ell^{EB}, \\ C_{\ell,\mathrm{obs}}^{TE} = \cos(2\beta) C_\ell^{TE} - \sin(2\beta) C_\ell^{TB}, \\ C_{\ell,\mathrm{obs}}^{EB} = \sin(4\beta)(C_\ell^{EE} - C_\ell^{BB})/2 + \cos(4\beta) C_\ell^{EB}, \\ C_{\ell,\mathrm{obs}}^{TB} = \sin(2\beta) C_\ell^{TE} + \cos(2\beta) C_\ell^{TB}. \end{cases}$$

$$\longrightarrow \quad C_{\ell,\mathrm{obs}}^{EB} = \tan(4\beta)(C_{\ell,\mathrm{obs}}^{EE} - C_{\ell,\mathrm{obs}}^{BB})/2.$$

hints of cosmic birefringence

$$\begin{cases} C_{\ell,\mathrm{obs}}^{TT} = C_\ell^{TT}, \\ C_{\ell,\mathrm{obs}}^{EE} = \cos^2(2\beta) C_\ell^{EE} + \sin^2(2\beta) C_\ell^{BB} - \sin(4\beta) C_\ell^{EB}, \\ C_{\ell,\mathrm{obs}}^{BB} = \cos^2(2\beta) C_\ell^{BB} + \sin^2(2\beta) C_\ell^{EE} + \sin(4\beta) C_\ell^{EB}, \\ C_{\ell,\mathrm{obs}}^{TE} = \cos(2\beta) C_\ell^{TE} - \sin(2\beta) C_\ell^{TB}, \\ C_{\ell,\mathrm{obs}}^{EB} = \sin(4\beta)(C_\ell^{EE} - C_\ell^{BB})/2 + \cos(4\beta) C_\ell^{EB}, \\ C_{\ell,\mathrm{obs}}^{TB} = \sin(2\beta) C_\ell^{TE} + \cos(2\beta) C_\ell^{TB}. \end{cases}$$

$$\longrightarrow \quad C_{\ell,\mathrm{obs}}^{EB} = \tan(4\beta)(C_{\ell,\mathrm{obs}}^{EE} - C_{\ell,\mathrm{obs}}^{BB})/2.$$

$$\beta = 0.35 \pm 0.14 \text{ (68\%CL)}$$

To be confirmed (or not) by future polarization observations!

Minami and Komatsu (2020) Phys. Rev. Lett. 125

HWP-induced miscalibration

Analytic $\widehat{C}_\ell$s satisfy the relations:

$$\begin{cases} \widehat{C}_\ell^{EB} \simeq \tan(4\widehat{\theta}) \left[\widehat{C}_\ell^{EE} - \widehat{C}_\ell^{BB}\right]/2 \\ \widehat{C}_\ell^{TB} \simeq \tan(2\widehat{\theta})\widehat{C}_\ell^{TE} \end{cases}$$

The HWP induces an additional miscalibration, **degenerate** with cosmic birefringence and polarization angle miscalibration!

Monelli et al. (2023) JCAP 03

HWP-induced miscalibration

Analytic $\widehat{C}_\ell$s satisfy the relations:

$$\begin{cases} \widehat{C}_\ell^{EB} \simeq \tan(4\widehat{\theta}) \left[\widehat{C}_\ell^{EE} - \widehat{C}_\ell^{BB}\right]/2 \\ \widehat{C}_\ell^{TB} \simeq \tan(2\widehat{\theta}) \widehat{C}_\ell^{TE} \end{cases}$$

our formulae suggest

$$\widehat{\theta} \equiv -\frac{1}{2} \arctan \frac{m_{qu} + m_{uq}}{m_{qq} - m_{uu}} \sim 3.8^\circ,$$

compatibly with simulations.

The HWP induces an additional miscalibration, **degenerate** with cosmic birefringence and polarization angle miscalibration!

This doesn't mean that the HWP will keep us from measuring β, but it shows how important it is to carefully calibrate $\mathcal{M}_{\mathrm{HWP}}$.

Monelli et al. (2023) JCAP 03

work in progress:
end-to-end model

including frequency dependence

For the single frequency model, we started from $d = (1\ 0\ 0) \cdot \mathcal{M}_{\mathsf{det}} \mathcal{R}_{\xi-\phi} \mathcal{M}_{\mathsf{HWP}} \mathcal{R}_{\phi+\psi} \cdot \mathsf{S}$, which can be generalized to account for the **frequency dependence** of $\mathcal{M}_{\mathsf{HWP}}$ and signal:

$$d^i = (1\ 0\ 0) \cdot \mathcal{M}_{\mathsf{det}} \mathcal{R}_{\xi-\phi} \int_{\nu^i_{\mathsf{min}}}^{\nu^i_{\mathsf{max}}} \frac{\mathrm{d}\nu}{\Delta\nu^i} \mathcal{M}_{\mathsf{HWP}}(\nu) \mathcal{R}_{\phi+\psi} \cdot \mathsf{S}^i(\nu)\,.$$

Additional generalizations (more components, beams and noise) are also easy to implement, and the resulting model can be used as a starting point to retrace the same steps as before.

modeling the multi-frequency maps

With HWP: $$\widehat{\mathsf{m}}^i \simeq \sum_\lambda \begin{pmatrix} g^i_\lambda & 0 & 0 \\ 0 & \rho^i_\lambda & \eta^i_\lambda \\ 0 & -\eta^i_\lambda & \rho^i_\lambda \end{pmatrix} \overline{\mathsf{m}}^i_\lambda(\nu) + \mathsf{n}^i \,,$$

where $$g^i_\lambda \equiv \int_{\nu^i_{\mathrm{min}}}^{\nu^i_{\mathrm{max}}} \frac{\mathrm{d}\nu}{\Delta\nu^i} a_\lambda(\nu) m_{\mathrm{ii}}(\nu)\,,$$

$$\rho^i_\lambda \equiv \frac{1}{2}\int_{\nu^i_{\mathrm{min}}}^{\nu^i_{\mathrm{max}}} \frac{\mathrm{d}\nu}{\Delta\nu^i} a_\lambda(\nu) \left[m_{\mathrm{qq}}(\nu) - m_{\mathrm{uu}}(\nu)\right]\,,$$

$$\eta^i_\lambda \equiv \frac{1}{2}\int_{\nu^i_{\mathrm{min}}}^{\nu^i_{\mathrm{max}}} \frac{\mathrm{d}\nu}{\Delta\nu^i} a_\lambda(\nu) \left[m_{\mathrm{qu}}(\nu) + m_{\mathrm{uq}}(\nu)\right]\,.$$

How the HWP non-idealities affect gain, polarization-efficiency and cross-pol leakage, differ for each frequency channel and each component.

work in progress with E. Komatsu, T. Matsumura, T. Ghigna and R. Takaku

moving forward

$$\{\widehat{\mathsf{m}}^i, \ldots, \widehat{\mathsf{m}}^{n_{\mathsf{chan}}}\} \quad \text{with} \quad \widehat{\mathsf{m}}^i \simeq \sum_\lambda \begin{pmatrix} g^i_\lambda & 0 & 0 \\ 0 & \rho^i_\lambda & \eta^i_\lambda \\ 0 & -\eta^i_\lambda & \rho^i_\lambda \end{pmatrix} \overline{\mathsf{m}}^i_\lambda(\nu) + \mathsf{n}^i\,.$$

work in progress with E. Komatsu, T. Matsumura, T. Ghigna and R. Takaku

moving forward

$$\{\widehat{\mathsf{m}}^{i}, \ldots, \widehat{\mathsf{m}}^{n_{\mathsf{chan}}}\} \quad \text{with} \quad \widehat{\mathsf{m}}^{i} \simeq \sum_{\lambda} \begin{pmatrix} g^{i}_{\lambda} & 0 & 0 \\ 0 & \rho^{i}_{\lambda} & \eta^{i}_{\lambda} \\ 0 & -\eta^{i}_{\lambda} & \rho^{i}_{\lambda} \end{pmatrix} \overline{\mathsf{m}}^{i}_{\lambda}(\nu) + \mathsf{n}^{i}\,.$$

↓ parametric or blind **component separation**
(HILC output can be modeled *analytically*)

FG-cleaned CMB map.

moving forward

$$\{\widehat{\mathsf{m}}^{i}, \ldots, \widehat{\mathsf{m}}^{n_{\mathsf{chan}}}\} \quad \text{with} \quad \widehat{\mathsf{m}}^{i} \simeq \sum_{\lambda} \begin{pmatrix} g^{i}_{\lambda} & 0 & 0 \\ 0 & \rho^{i}_{\lambda} & \eta^{i}_{\lambda} \\ 0 & -\eta^{i}_{\lambda} & \rho^{i}_{\lambda} \end{pmatrix} \overline{\mathsf{m}}^{i}_{\lambda}(\nu) + \mathsf{n}^{i}\,.$$

↓ parametric or blind **component separation**
(HILC output can be modeled *analytically*)

FG-cleaned CMB map.

↓ **likelihood maximization**

Estimates of r and/or β.

work in progress with E. Komatsu, T. Matsumura, T. Ghigna and R. Takaku

conclusions and outlook

- Much information is still hidden in CMB polarization, for instance **primordial B-modes** and **cosmic birefringence** as probes of, respectively, inflationary and parity-violating physics,
- New physics can be probed only if systematics are well under control,
- A rotating HWP can help, but it induces additional systematics which should be accounted for (**HWP-induced miscalibration**),

- We are now provided with an analytical model and a simulation pipeline that can be used to study the impact of the HWP in more realistic scenarios. this is key for the planning of the next generation of CMB experiments.

backup

sketch of the pipeline

beamconv: convolution code simulating TOD for CMB experiments with realistic polarized **beams**, scanning strategies and **HWP**.

DUCC: collection of basic programming tools for numerical computation: `fft`, `sht`, `healpix`, `totalconvolve`...

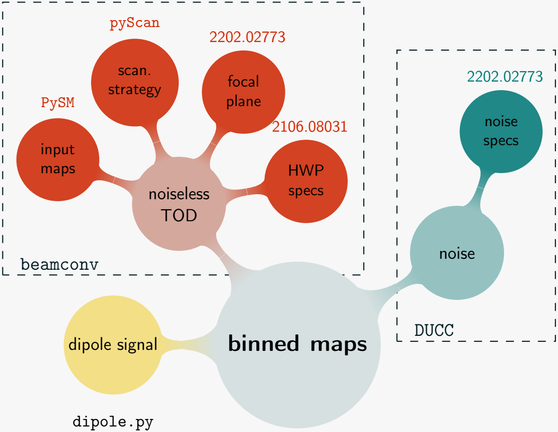

github.com/AdriJD/beamconv, A. Duivenvoorden et al "2012.10437", gitlab.mpcdf.mpg.de/mtr/ducc

input maps

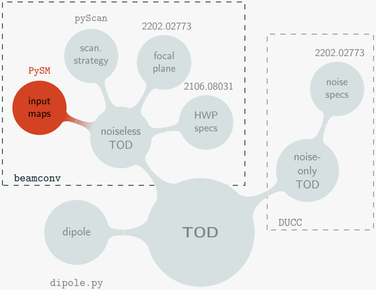

The pipeline can be fed with arbitrary input maps: CMB, foregrounds, or both.

In the paper: I, Q and U input maps with $n_{\mathrm{side}} = 512$ from best-fit 2018 Planck power spectra;

scanning strategy

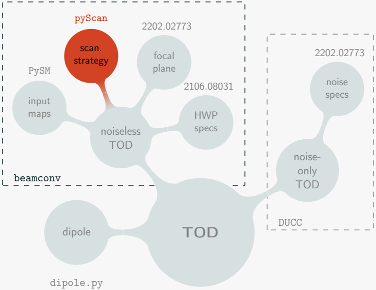

The pipeline can read or calculate pointings. We implemented some functionalities of `pyScan` in `beamconv` to deal with satellite missions.

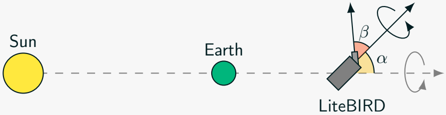

In the paper: 1 year of LiteBIRD-like scanning strategy.

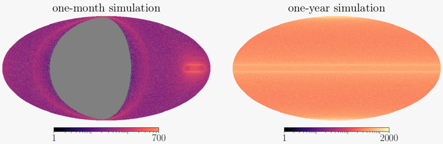

https://github.com/tmatsumu/LB_SYSPL_v4.2

focal plane specifics

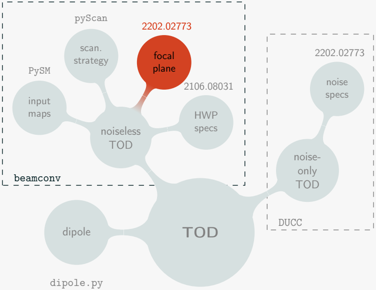

The pipeline can read from the Instrument Model Database (IMO):

```
{'name': 'M02_030_QA_140T',
 'wafer': 'M02',
 'pixel': 30,
 'pixtype': 'MP1',
 [...]
 'pol': 'T',
 'orient': 'Q',
 'quat': [1, 0, 0, 0]}
```

In the paper: 160 dets from M1-140.

specs.	values
f_{samp}	19 Hz
HWP rpm	39
FWHM	30.8 arcmin
offset quats.	[...]

HWP specifics

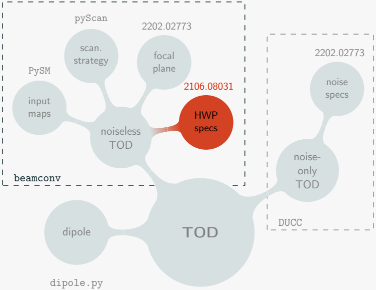

In the paper: HWP is assumed to be ideal in the **first** simulation run (ideal TOD) and realistic in the **second** (non-ideal TOD).

Realistic HWP Mueller matrix elements as shown previously:

$\mathcal{M}_{\text{HWP}} =$

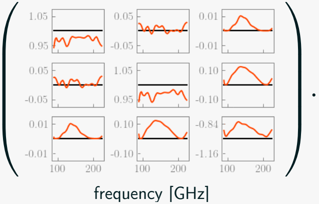

ideal vs non-ideal output spectra (1)

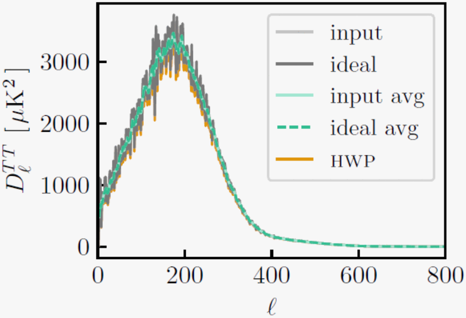

(beam transfer function not deconvolved)

- TT leaked a bit

ideal vs non-ideal output spectra (1)

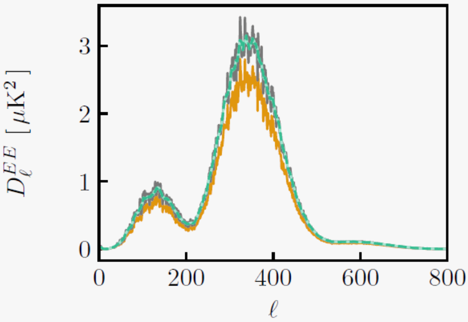

(beam transfer function not deconvolved)

- *TT* leaked a bit
- *EE* leaked a lot!

ideal vs non-ideal output spectra (1)

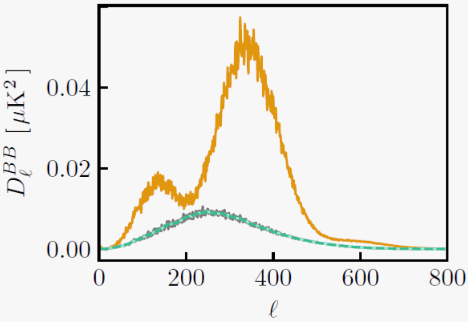

(beam transfer function not deconvolved)

- *TT* leaked a bit
- *EE* leaked a lot!
- *BB* larger (*EE* shape!)

ideal vs non-ideal output spectra (1)

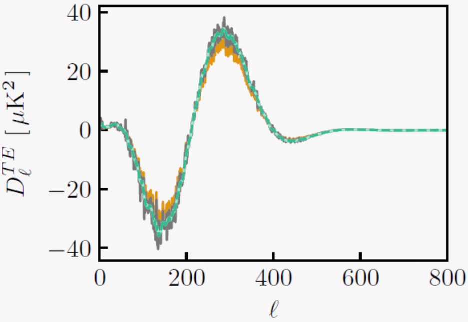

(beam transfer function not deconvolved)

- *TT* leaked a bit
- *EE* leaked a lot!
- *BB* larger (*EE* shape!)
- *TE* leaked a bit

ideal vs non-ideal output spectra (1)

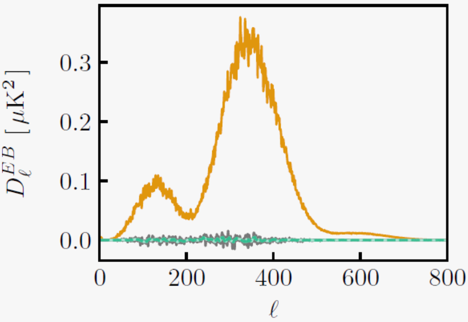

(beam transfer function not deconvolved)

- *TT* leaked a bit
- *EE* leaked a lot!
- *BB* larger (*EE* shape!)
- *TE* leaked a bit
- *EB* non-zero!

ideal vs non-ideal output spectra (1)

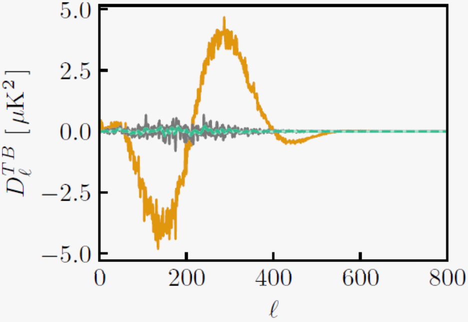

(beam transfer function not deconvolved)

- *TT* leaked a bit
- *EE* leaked a lot!
- *BB* larger (*EE* shape!)
- *TE* leaked a bit
- *EB* non-zero!
- *TB* non-zero!

ideal vs non-ideal output spectra (2)

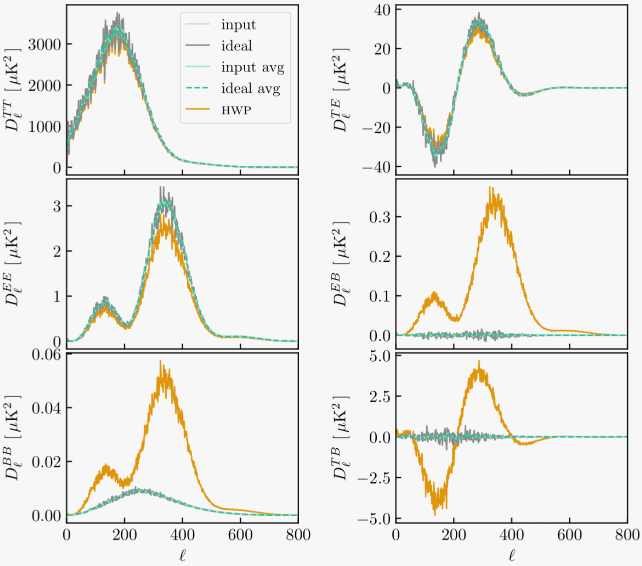

why “cosmic birefringence”?

Birefringence: property of a material whose refractive index depends on the polarization and propagation direction of light.

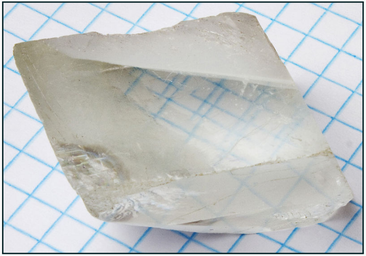

Thinner slabs, normal incidence:
no double refraction, only retardance.

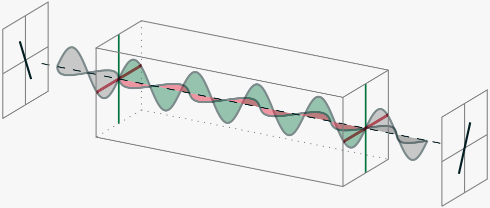

Both optical and cosmic birefringence rotate polarization vectors.

instrument miscalibration

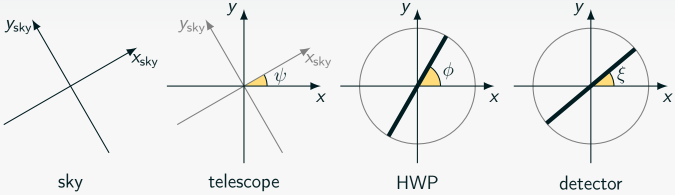

So far, we assumed $\begin{cases} \widehat{\psi} \equiv \psi, \\ \widehat{\phi} \equiv \phi, \\ \widehat{\xi} \equiv \xi, \end{cases}$ but more generally $\begin{cases} \widehat{\psi} \equiv \psi + \delta\phi, \\ \widehat{\phi} \equiv \phi + \delta\psi, \\ \widehat{\xi} \equiv \xi + \delta\xi. \end{cases}$

Taking such (frequency-independent) deviations into account:

$$\widehat{\theta} = -\frac{1}{2} \arctan \frac{\langle m_{qu} + m_{uq} \rangle}{\langle m_{qq} - m_{uu} \rangle} + \delta\theta, \qquad \text{where } \delta\theta \equiv \delta\xi - \delta\psi - 2\delta\phi.$$